BioArchitecture 2:5, 171–174; September/October 2012; © 2012 Landes Bioscience

Competition and compensation

Dissecting the biophysical and functional differences between the class 3 myosin paralogs, myosins 3a and 3b

Uri Manor,[1,†,*] M'hamed Grati,[1] Christopher M. Yengo,[2] Bechara Kachar[1] and Nir S. Gov[3]

[1]Laboratory of Cell Structure and Dynamics; National Institute on Deafness and Other Communication Disorders; National Institutes of Health; Bethesda, MD USA; [2]Department of Cellular and Molecular Physiology; Penn State College of Medicine; Hershey, PA USA; [3]Department of Chemical Physics; Weizmann Institute of Science; Rehovot, Israel

[†]Current affiliation: Section on Organelle Biology; National Institute of Child Health and Human Development; National Institutes of Health; Bethesda, MD USA

Stereocilia are actin protrusions with remarkably well-defined lengths and organization. A flurry of recent papers has reported multiple myosin motor proteins involved in regulating stereocilia structures by transporting actin-regulatory cargo to the tips of stereocilia.[1-13] In our recent paper, we show that two paralogous class 3 myosins—Myo3a and Myo3b—both transport the actin-regulatory protein Espin 1 (Esp1) to stereocilia and filopodia tips in a remarkably similar, albeit non-identical fashion.[1] Here we present experimental and computational data that suggests that subtle differences between these two proteins' biophysical and biochemical properties can help us understand how these myosin species target and regulate the lengths of actin protrusions.

Keywords: myosin, actin, filopodia, cytoskeleton, motor proteins, stereocilia, deafness

Submitted: 07/23/12

Accepted: 08/03/12

http://dx.doi.org/10.4161/bioa.21733

*Correspondence to: Uri Manor; Email: manoru@mail.nih.gov

Commentary to: Merritt RC, Manor U, Salles FT, Grati M, Dose AC, Unrath WC, et al. Myosin IIIB uses an actin-binding motif in its espin-1 cargo to reach the tips of actin protrusions. Curr Biol 2012; 22:320–5; PMID:22264607; http://dx.doi.org/10.1016/j.cub.2011.12.053.

MYO3A has been implicated in late onset hearing loss in humans and mice.[14] Recent studies showed that myosin IIIA (Myo3a) targets the deafness-associated actin-binding protein Esp1[15] to the tips of actin protrusions.[3,16] These two proteins synergistically interact such that Myo3 motor activity helps concentrate Esp1 at actin filament barbed-ends, while Esp1 WH2 activity enhances actin polymerization, thereby increasing steady-state filament (and therefore actin protrusion) lengths.[3] The late-onset hearing loss phenotype associated with mutations in *MYO3A* led us to hypothesize that the *MYO3A* paralog, *MYO3B*, could be partially compensating for MYO3A. One key difference between Myo3a and Myo3b is that Myo3b lacks an actin-binding site in its tail that is essential for its ability to target the tips of actin protrusions.[17] Interestingly, Myo3b and Myo3a constructs lacking the actin-binding tail domain (THDII) can still target the tips of actin protrusions in the presence of Esp1, and this rescue of tip-localization is dependent on the C-terminus actin-binding site in Esp1.[1]

The observation that unlike Myo3a, Myo3b can only localize to the tips of stereocilia when associated with Esp1,[1] led us to further investigate how these proteins behave when all three are coexpressed in a heterologous system. We found that when Myo3a, Myo3b, and Esp1 are coexpressed in COS7 cells, Myo3a invariably accumulated at the tips of filopodia in a steep tip-to-base gradient, while Myo3b localized to filopodia tips proximally to Myo3a with a much shallower tip-to-base gradient along the shafts of filopodia. We also found that inversely proportional amounts of the two myosins were found in the overlapping regions near the tips of filopodia, strongly suggestive of competition between the two proteins for localization to the same compartment (**Fig. 1**).

In order to test whether the differential myosin distributions were the result of differences in the tail vs. the motor actin-binding domains of the two isoforms, we also performed cotransfections with Myo3aΔTHDII, Myo3b, and Esp1, as well as Myo3aΔTHDII, Myo3a, and

©2012 Landes Bioscience. Do not distribute.

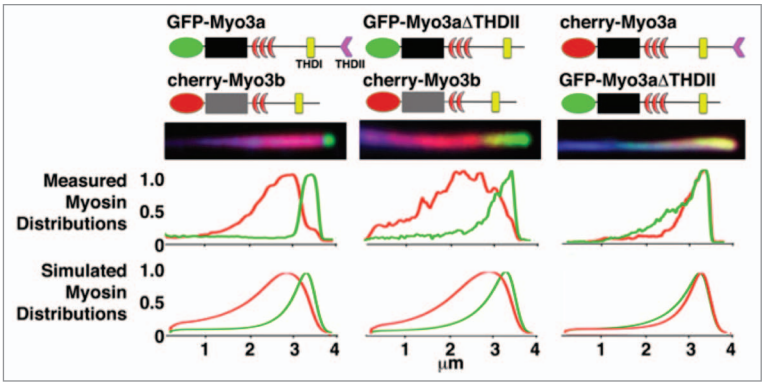

Figure 1. Filopodia from COS7 cells co-expressing GFP-Myo3a and cherry-Myo3b consistently display GFP-Myo3a accumulated at their extreme tips, while cherry-Myo3b consistently trails behind Myo3a with a relatively longer tip-to-base decay length (left column). GFP-Myo3a with and without the 3THDII actin-binding site (GFP-Myo3aΔTHDII) consistently accumulates at filopodia tips ahead of GFP-Myo3b (left and middle columns, respectively), while GFP-Myo3a does not exclude GFP-Myo3aΔTHDII (right column). The black and gray boxes are the motor domains of Myo3a and Myo3b, respectively. The red crescents represent the IQ domains.

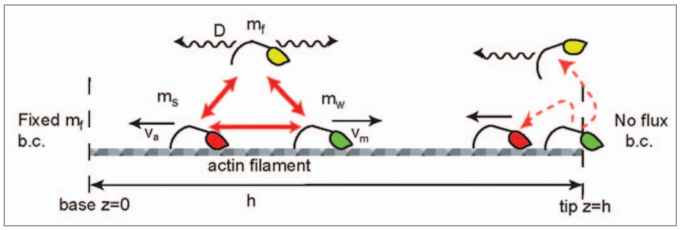

Figure 2. Schematic description of the calculated model of myosin distributions. We consider freely diffusing (yellow), processively walking (green) and stalled (red) myosins, that convert into each other (red arrows) with defined reaction coefficients. At the protrusion tip we illustrate the two types of boundary conditions that we used; walking motors detach and diffuse freely from the tip, or become stalled and are carried away by the actin treadmilling.

Esp1 (**Fig. 1**). We found that, like Myo3a, Myo3aΔTHDII excluded Myo3b from filopodia tips. In contrast, we found that Myo3aΔTHDII was not excluded from filopodia tips when transfected with Myo3a. Finally, we also observed that Myo3aΔTHDII appeared to have a longer decay length than Myo3a in its tip-to-base gradient distribution, somewhat similar to Myo3b (**Fig. 1**).

To gain further insight into which factors determine the distributions for the different Myo3:Esp1 complexes, we generated a computational model based on continuum equations to describe the distribution of myosin motors along a one-dimensional protrusion [4]. The motors are described to be in one of three states: freely diffusing (m_f), moving ("walking") processively toward the tip (m_w) at velocity v_m, or bound to the actin but stalled and therefore moving toward the protrusion base (m_s) at the treadmilling velocity of the actin (v_a). This model is schematically shown in **Figure 2**.

The dynamical equations are given by:

$$\frac{\partial m_f}{\partial t} = D\nabla^2 m_f + k_{off} m_w + k_{off,b} m_s - \left(k_{on} + k_{on,b}\right) m_f \left(1 - (m_w + m_s)\right)$$

$$\frac{\partial m_w}{\partial t} = -(v_m - v_a)\nabla m_w + k_{off,sw}(1 + K(m_w + m_s)^{\beta}) m_w + k_{on,sw} m_s + k_{on} m_f (1 - (m_w + m_s)) - k_{off} m_w$$

$$\frac{\partial m_s}{\partial t} = v_a \nabla m_s + k_{off,bw}(1 + K(m_w + m_s)^{\beta}) m_w - k_{on,sw} m_s - k_{on} m_f (1 - (m_w + m_s))$$

where D is the diffusion coefficient of the free myosin, and K is the coefficient describing the process whereby walking myosins become stalled due to interaction with fellow actin-bound myosins (stalled or walking). This interaction term could be due to "traffic-jam" effects as well as biochemical events, such as Myo3a outcompeting Myo3b in binding to Esp1. The power β in this interaction term describes the cooperative nature of these processes. We chose the parameters in **Table 1** below, while all the other parameters remained unchanged and listed below. We also take into account in **Equation 1** the excluded-volume effects between actin-bound motors.

The boundary conditions we chose are of a constant concentration of myosins at the base of the protrusion, where there is contact with the large reservoir of the cell cytoplasm, and of zero-flux at the closed tip. Walking myosins that reach the tip are assumed either to fall off the actin filaments and become freely diffusing, or to become "stalled," whereupon they remain bound to the actin core which is slowly moving back toward the base due to retrograde flow and actin treadmilling. We tested these two different choices, and found that the best overall agreement for all the different experiments was captured by the boundary condition of myosins detaching at the tip.

The situation in the case of two different Myo3 species shown in **Figure 1** is more complicated, since we now have to consider two sets of equations of the form of Equation 1. We expect that the actin-binding affinity of Myo3b is lower than that of Myo3a due to the lack of an actin-binding tail in Myo3b. This should in theory decrease the overall actin-binding affinity of Myo3b. Furthermore, we also know from in vitro experiments that the motor domain of Myo3b has a lower affinity for actin as well. Given the ~50% reduction in ATPase and ADP-release rates for Myo3b along with our kymograph data showing ~2× faster tip-directed velocities for Myo3a vs. Myo3b,[1] we defined the Myo3b tip-directed velocity to be about half that of Myo3a. We first checked if these differences alone are enough to explain the distributions shown in **Figure 1**, and we found that we could not get any agreement in terms of the mutually exclusive localization of Myo3a vs. Myo3b.

©2012 Landes Bioscience. Do not distribute.

From this we concluded that there must be some form of direct interaction (beyond the excluded volume effect) between the myosin species. The most obvious form of interaction to consider was that walking Myo3b could stall much more readily than Myo3a when the two proteins collide, perhaps by having its Esp1 cargo stolen by neighboring Myo3a molecules. We included this effect (*K* term in Equation 1), so that this term becomes (for the dynamics of the walking Myo3b):

$$-k_{offsw}(1 + K(m_{w,a} + m_{s,a})^{\hat{a}})m_{w,b}$$

where the second subscript denotes the type of Myo3. With this description we were able to reproduce the main qualitative characteristics of the distributions shown in **Figure 1**. Interestingly, since Myo3aΔTHDII is not excluded from filopodia tips in the presence of Myo3a, our results predict that the Myo3a THDI has a higher affinity for Esp1 than the Myo3b THDI. Future experiments will be able to determine whether this prediction is correct, which we believe to be likely, especially considering that the Myo3a THDI sequence is significantly different from the Myo3b THDI sequence.[18] This demonstrates the utility of this theoretical modeling approach in providing insight that can guide future experiments.

It should be noted that these distributions are not precise fits. It's important to consider that all of the interactions between the motors have been lumped into the single *K* term in our analysis for simplicity's sake. Furthermore, even within the simplified assumptions made in this study, we have not exhausted all of the regimes of solutions possible within the confines of the current model. Nonetheless, we found that changing these key parameters for each myosin construct allowed us to qualitatively reproduce the main features we observed in these distributions—namely, the longer tip-to-base decay length for Myo3b and Myo3aΔTHDII (controlled by reducing their k_{on} and by increasing their tendency to stall or fall off), and the exclusion of Myo3b from the filopodia tips in the presence of Myo3a (which is controlled by making Myo3a able to outcompete Myo3b for Esp1 cargo binding, thereby rendering Myo3b unable to walk toward the tip). Future experimental and computational studies will have to be done to attempt to dissect the details of the contributions of different interaction terms.

Table 1. Parameters used for simulations

	v_m (μm/sec)	k_{on} (sec^{-1} concentration^{-1})	*K* (concentration^{-1})	β
Myo3aΔK	0.075	1	0	0
Myo3bΔK	0.05	0.5	5000	1
Myo3aΔTHDII	0.075	0.5	0	1

$k_{off} = k_{offs} = k_{off}$sw = 0.1sec^{-1}, k_{on}sw = 1sec^{-1}concentration^{-1}, k_{on}s = 0.1sec^{-1}concentration^{-1}, and the concentration of free myosins in the bulk (protrusion base) was taken to be: mf = 0.0001 in arbitrary units of concentration (the final plots in Figure 1 give relative concentration with respect to the peak value). The treadmilling velocity of actin was taken to be: v_a = 0.01 (μm/sec). We convoluted all of our calculated distributions with a 50 nm wide Gaussian function to account for our finite optical resolution.

It is intriguing that Myo3a elongates Esp1 filopodia about twice as much as Myo3b. Our results strongly suggest that the different biophysical and biochemical properties of these two paralogous motor proteins are directly related to their proportionally dissimilar filopodia elongation activities. Specifically, we believe that the filopodia elongation activity of class 3 myosins is directly proportional to their tip-directed velocities. The direct proportionality between the tip-directed velocities of Myo3a vs. Myo3b and the lengths of Myo3a vs. Myo3b filopodia is strongly suggestive, and is inherently logical: A faster motor gives rise to a larger flux of cargo proteins to the tip, which should result in greater polymerization activity[6] and/or a greater flux of actin monomers,[19] depending on the context or cargo of these motors. For example, since Esp1 has both crosslinking activity as well as actin-polymerization activity,[3,20] a larger flux of such a protein near actin barbed-ends could enable a faster rate of actin polymerization and/or a more highly cross-linked actin bundle, which in turn can produce a longer protrusion.[19] Furthermore, our earlier studies demonstrated that Myo3a N-terminal kinase activity modulates Myo3a motor and elongation activity, since autophosphorylation of the motor domain by the Myo3a kinase domain lowers the motor domain's ATPase rate.[16,21] Taken together, all of our observations point toward a direct relationship between the efficiency of motor-dependent tip-targeting of actin-regulatory cargo and actin protrusion lengths.

In summary, through our combination of experimental and computational approaches, we were able to dissect the underlying molecular components of these myosin:cargo dynamics. This work demonstrates the intricate nature of the interactions between molecular motors within cellular protrusions, and the usefulness of theoretical modeling in deciphering them. Specifically, we can begin to ask and answer detailed questions about the contribution of different aspects of myosin motility, (e.g., actin-binding and motor activity), to not only their biophysical behavior, but also their physiological function. Indeed, these results strongly indicate that Myo3b can behave quite similarly to Myo3a, but they also show that Myo3b "falls short" of Myo3a activity in terms of elongation activity. This finding is one plausible explanation for the late-onset phenotype associated with mutations in *MYO3A*. Overall, these studies lend stronger support for further exploring the potential role for Myo3b in compensating for Myo3a, and how these two motor proteins interact in a physiological context.

Disclosure of Potential Conflicts of Interest

No potential conflicts of interest were disclosed.

Acknowledgements

C.M.Y. is supported by NIH EY018141.

©2012 Landes Bioscience. Do not distribute.

References

1. Merritt RC, Manor U, Salles FT, Grati M, Dose AC, Unrath WC, et al. Myosin IIIB uses an actin-binding motif in its espin-1 cargo to reach the tips of actin protrusions. Curr Biol 2012; 22:320-5; PMID:22264607; http://dx.doi.org/10.1016/j.cub.2011.12.053
2. Manor U, Disanza A, Grati M, Andrade L, Lin H, Di Fiore PP, et al. Regulation of stereocilia length by myosin XVa and whirlin depends on the actin-regulatory protein Eps8. Curr Biol 2011; 21:167-72; PMID:21236676; http://dx.doi.org/10.1016/j.cub.2010.12.046
3. Salles FT, Merritt RC Jr., Manor U, Dougherty GW, Sousa AD, Moore JE, et al. Myosin IIIa boosts elongation of stereocilia by transporting espin 1 to the plus ends of actin filaments. Nat Cell Biol 2009; 11:443-50; PMID:19287378; http://dx.doi.org/10.1038/ncb1851
4. Rzadzinska AK, Nevalainen EM, Prosser HM, Lappalainen P, Steel KP. MyosinVIIa interacts with Twinfilin-2 at the tips of mechanosensory stereocilia in the inner ear. PLoS One 2009; 4:e7097; PMID:19774077; http://dx.doi.org/10.1371/journal.pone.0007097
5. Sakaguchi H, Tokita J, Naoz M, Bowen-Pope D, Gov NS, Kachar B. Dynamic compartmentalization of protein tyrosine phosphatase receptor Q at the proximal end of stereocilia: implication of myosin VI-based transport. Cell Motil Cytoskeleton 2008; 65:528-38; PMID:18412156; http://dx.doi.org/10.1002/cm.20275
6. Naoz M, Manor U, Sakaguchi H, Kachar B, Gov NS. Protein localization by actin treadmilling and molecular motors regulates stereocilia shape and treadmilling rate. Biophys J 2008; 95:5706-18; PMID:18936243; http://dx.doi.org/10.1529/biophysj.108.143453
7. Manor U, Kachar B. Dynamic length regulation of sensory stereocilia. Semin Cell Dev Biol 2008; 19:502-10; PMID:18692583; http://dx.doi.org/10.1016/j.semcdb.2008.07.006
8. Schneider ME, Dosé AC, Salles FT, Chang W, Erickson FL, Burnside B, et al. A new compartment at stereocilia tips defined by spatial and temporal patterns of myosin IIIa expression. J Neurosci 2006; 26:10243-52; PMID:17021180; http://dx.doi.org/10.1523/JNEUROSCI.2812-06.2006
9. Belyantseva IA, Boger ET, Naz S, Frolenkov GI, Sellers JR, Ahmed ZM, et al. Myosin-XVa is required for tip localization of whirlin and differential elongation of hair-cell stereocilia. Nat Cell Biol 2005; 7:148-56; PMID:15654330; http://dx.doi.org/10.1038/ncb1219
10. Rzadzinska AK, Schneider ME, Davies C, Riordan GP, Kachar B. An actin molecular treadmill and myosins maintain stereocilia functional architecture and self-renewal. J Cell Biol 2004; 164:887-97; PMID:15024034; http://dx.doi.org/10.1083/jcb.200310055
11. Belyantseva IA, Boger ET, Friedman TB. Myosin XVa localizes to the tips of inner ear sensory cell stereocilia and is essential for staircase formation of the hair bundle. Proc Natl Acad Sci U S A 2003; 100:13958-63; PMID:14610277; http://dx.doi.org/10.1073/pnas.2334417100
12. Anderson DW, Probst FJ, Belyantseva IA, Fridell RA, Beyer L, Martin DM, et al. The motor and tail regions of myosin XV are critical for normal structure and function of auditory and vestibular hair cells. Hum Mol Genet 2000; 9:1729-38; PMID:10915760; http://dx.doi.org/10.1093/hmg/9.12.1729
13. Mogensen MM, Rzadzinska A, Steel KP. The deaf mouse mutant whirler suggests a role for whirlin in actin filament dynamics and stereocilia development. Cell Motil Cytoskeleton 2007; 64:496-508; PMID:17326148; http://dx.doi.org/10.1002/cm.20199
14. Walsh VL, Raviv D, Dror AA, Shahin H, Walsh T, Kanaan MN, et al. A mouse model for human hearing loss DFNB30 due to loss of function of myosin IIIA. Mamm Genome 2011; 22:170-7; PMID:21165622; http://dx.doi.org/10.1007/s00335-010-9310-6
15. Zheng L, Sekerková G, Vranich K, Tilney LG, Mugnaini E, Bartles JR. The deaf jerker mouse has a mutation in the gene encoding the espin actin-bundling proteins of hair cell stereocilia and lacks espins. Cell 2000; 102:377-85; PMID:10975527; http://dx.doi.org/10.1016/S0092-8674(00)00042-8
16. Quintero OA, Moore JE, Unrath WC, Manor U, Salles FT, Grati M, et al. Intermolecular autophosphorylation regulates myosin IIIa activity and localization in parallel actin bundles. J Biol Chem 2010; 285:35770-82; PMID:20826793; http://dx.doi.org/10.1074/jbc.M110.144360
17. Les Erickson F, Corsa AC, Dose AC, Burnside B. Localization of a class III myosin to filopodia tips in transfected HeLa cells requires an actin-binding site in its tail domain. Mol Biol Cell 2003; 14:4173-80; PMID:14517327; http://dx.doi.org/10.1091/mbc.E02-10-0656
18. Katti C, Dalal JS, Dosé AC, Burnside B, Battelle BA. Cloning and distribution of myosin 3B in the mouse retina: differential distribution in cone outer segments. Exp Eye Res 2009; 89:224-37; PMID:19332056; http://dx.doi.org/10.1016/j.exer.2009.03.011
19. Zhuravlev PI, Lan Y, Minakova MS, Papoian GA. Theory of active transport in filopodia and stereocilia. Proc Natl Acad Sci U S A 2012; 109:10849-54; PMID:22711803; http://dx.doi.org/10.1073/pnas.1200160109
20. Loomis PA, Kelly AE, Zheng L, Changyaleket B, Sekerková G, Mugnaini E, et al. Targeted wild-type and jerker espins reveal a novel, WH2-domain-dependent way to make actin bundles in cells. J Cell Sci 2006; 119:1655-65; PMID:16569662; http://dx.doi.org/10.1242/jcs.02869
21. Salles FT, Merritt RC Jr., Manor U, Dougherty GW, Sousa AD, Moore JE, et al. Myosin IIIa boosts elongation of stereocilia by transporting espin 1 to the plus ends of actin filaments. Nat Cell Biol 2009; 11:443-50; PMID:19287378; http://dx.doi.org/10.1038/ncb1851

©2012 Landes Bioscience. Do not distribute.